

Design Optimization of Axial Flux Permanent Magnet (AFPM) motor using Metaheuristic Golden Eagle Optimizer-(GEO) algorithm.

Mamidi Ramakrishna Rao

Design Engineering Consultant, DHI-QUEST Private Ltd, Hyderabad, India
mamidimr@gmail.com, mamidimr@dhi-quest.com

ABSTRACT

The choice of motor used in electric vehicles is an important decision. In motor selection, simple design, high power density, low maintenance cost, and easy controllability, features come to the fore. Different types of motors namely DC motors, Induction motors, Reluctance motors, Permanent magnet motors are being used. With recent developments, permanent magnet motors, in particular, axial-flux-permanent-magnet (AFPM) motors are gaining considerable preference. In this paper, power density optimization of AFPM motor is done using Metaheuristic optimization method namely "Golden Eagle Optimizer". For design and optimization, the necessary basic specifications and coefficients are taken from a model "Nissan-Leaf 2015". For design optimization, optimization the tool is taken from "matlabcentral-fileexchange-84430-golden-eagle-optimizer." The results are analyzed and discussed. The work can be extended to other versions of APFM motors with multiple objectives.

Date of Submission: 23-02-2024

Date of acceptance: 04-03-2024

I. INTRODUCTION

In the Electrical Vehicle's traction system, there are seven types of motors in use. They are Brushed DC motor (Used in Fiat Panda Elettra), Brushless DC motor (BLDC) (Used in Toyota Prius), Permanent Magnet Synchronous Motor (PMSM) (Used in Chevrolet Bolt EV, BMW i3), Ford Focus Electric), Nissan Leaf, Induction motor (used in Tesla Model S, Toyota RAV 4 and GM EV1), Switched Reluctance Motor (SRM), Synchronous Reluctance Motor, and advanced motor -Axial Flux Permanent Magnet Motor (used in Renovo Coupe). Each type of motor has strengths and weaknesses.

However, when high efficiency and high-power density are needed, Permanent magnet motors are most suitable choice. The power density comparison of different motor types currently used in EVs is given in page 5 of ref [1].

Axial flux permanent magnet (AFPM) synchronous machines performance and dimensions fit very well in electrical-vehicles-requirements. They satisfy the major requirements like high-torque-density, low cogging-torques and higher efficiency. Manufacturers like FIAT, Porche, Volvo, Kia, Jaguar, Skoda and Hyundai, in some of their car models, use Permanent Magnet motors.

In this paper, a metaheuristic optimization method namely "Golden Eagle Optimization" is used to reduce the active material content of AFPM machines for a given amount of torque.

The two basic parameters, namely nominal power and nominal torque are worked out from vehicle specifications, maximum speed, maximum acceleration, maximum slope together with vehicle characteristics. For vehicle specifics, Nissan-Leaf 2015 electric car specifications, is considered. [2] The specifications are shown in table1 and 2.

II. ANALYSIS

2.1. POWER AND TORQUE

Consider a vehicle moving at a velocity 'v' on a road having a slope. The forces acting are gravitational, inertia, aerodynamic resistive and rolling resistance. The nominal power (Pn) and the torque (Tn) required to move the vehicle to maximum speed is calculated using the formula below and ref [3]

$$F_t = (F_g + F_r + F_d + F_a). \quad (1)$$

F_t = Total tractive force

F_g = Parallel component of gravitational force.

F_r = Rolling resistance force

$$F_d = \text{aerodynamic drag resistance force}$$

$$F_a = \text{Acceleration force}$$

$$F_t = \frac{M_v}{\eta_{tr}} \cdot g \cdot \sin \alpha + M_v \cdot g \cdot C_r \cdot \cos \alpha + (1/2) \cdot \rho_a \cdot C_d \cdot A_v \cdot (V_v + V_{air})^2 + \delta \cdot M_v \cdot (dV_v/dt)$$

(2)

M_v = Vehicle mass
 g = gravity coefficient
 α = slope of the road
 $P_n = (1/\eta_{tr}) \cdot V_{vm} \cdot F_t$

(3)

P_n = Traction power of the motor
 η_{tr} = Transmission efficiency.
 V_{vm} = Maximum velocity

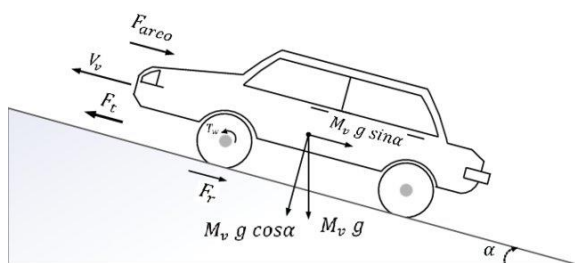


Fig. 1. Forces acting on moving vehicle [3]

Table I	
VEHICLE'S SPECIFICATIONS [2]	
Parameter [unit]	Value
Gross mass [kg]	1645
Maximum velocity [km/h]	144
Maximum acceleration [km/h/sec]	100/11.5
Distance for one charging cycle [km]	160
Wheel radius [m]	0.315
Transmission ratio	8.19
Frontal area [m ²]	2
Axle moment of inertia [kg/m ²]	3

Following detailed equations in ref [3], a nominal power of 80 kW and nominal torque 254 Nm with base speed of 3000rpm and speed ratio (Maximum speed / base speed) of 3.3 is chosen for further analysis and optimization.

2.2 APFM Motors

APFM motors have many topologies. They are single-sided, double sided, internal stator, multi-staged structures. A single-gap axial flux slotted machine with sinusoidal permanent magnets is considered for analysis.

Table II	
VEHICLE'S COEFFICIENTS [2]	
Parameter[unit]	Value
Rolling resistance	0.0083
Air density [kg/m ²]	1.2
Aerodynamic coefficient	0.28
Transmission efficiency	0.96
Air velocity [km/h]	12
Inverter efficiency	0.95
Motor efficiency	0.95

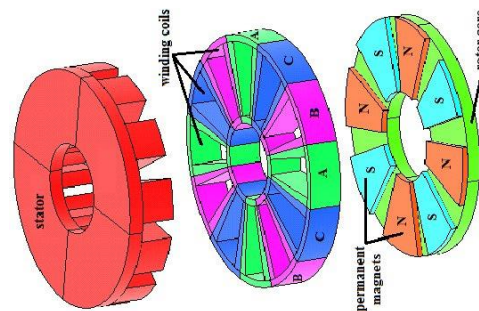


Fig 2. View of single sided AFPM machine [4]

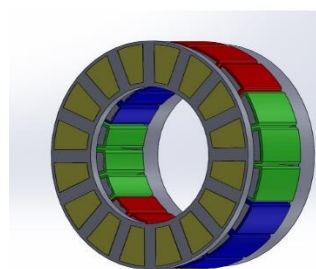


Fig 3. View of single sided wound AFPM machine [5]

2.3 Golden Eagle Optimization (GEO) principle

A population-based heuristics optimizer “Golden Eagle Optimizer algorithm” is used for optimization. The principle of GEO is explained below:

Golden eagles leverage their agility and speed with remarkable precision in the pursuit of prey, earning them a position of mystic reverence in the natural world. Their standard cruising speed ranges from 45 to 52 km/h. However, when homing in on prey, their velocity dramatically escalates. During a direct dive, the velocity reaches an astonishing 190 km/h. This remarkable hunting ability is complemented by their

extraordinary vision, allowing them to identify potential prey from considerable distances, even while in mid-flight. Eagles possess binocular vision, a feature that enables them to focus on a single object with both eyes, enhancing their depth perception and contributing to the precision of their attacks. They have four noteworthy features while hunting for their prey.

- 1) The first feature is “Spiral trajectory” for search and “straight” path for attack.
- 2) The second feature is – “smooth transition to more propensity to attack”.
- 3) The third feature is “they retain for both cruise and attack in every moment of flight”.
- 4) The fourth feature is “they look for other eagles’ information on prey”.

The intelligence of golden eagles (Fig 4) reveals their ability to fine tune their speed during hunting process. This behavior has been adopted in mathematical modelling reflecting in exploration and exploitation employed in global optimization methods. Their search pattern follows a spiral trajectory, (exploration), while a direct, linear path characterizes their approach during the attack phase (Fig 5)

The transition from exploration to exploitation begins with a low attack coefficient (P_a) and high cruise coefficient (P_c). During the progress of iterations, (P_a) gradually increases, and (P_c) decreases. Intermediate values can be calculated using the linear transition displayed below in equation (4 and 5)

$$p_a = p_a^o + \frac{t}{T}(p_a^T - p_a^o). \quad (4)$$

$$p_c = p_c^o + \frac{t}{T}(p_c^T - p_c^o). \quad (5)$$

Where t indicates current iteration and T indicates maximum iteration. p_a^o and p_a^T are the initial and final values for propensity to attack. Mathematical implementation of Cruise (exploration), attack (exploitation), moving to new positions are explained in detail in “Golden Eagle Optimizer: A nature inspired metaheuristic algorithm” [6][7] and therefore are not repeated here.



Fig. 4 Golden Eagle

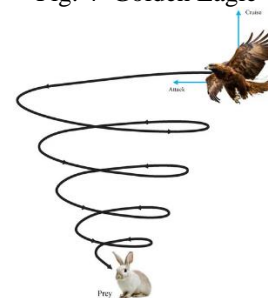


Fig. 5 Cruise and attack of Golden Eagle’s prey.

Table III	
Parameter values set in GEO algorithm	
Parameter	Value
Population size	100
Iterations (maximum)	1000
Propensity to Attack vector (Initial/Final)	0.5/2.0
Propensity to Cruise vector (Initial/ Final)	1/0.5

Algorithm 1. Pseudo-code of GEO [6]

```

Initialize the population of golden eagles.
Evaluate fitness function.
Initialize population memory.
Initialize  $p_a$  and  $p_c$ .
for each iteration  $t$ 
    Update  $p_a$  and  $p_c$ .
    for each golden eagle  $i$ 
        Randomly select a prey from the
        population’s memory
        Calculate attack vector  $A^*$ .
        if attack vector’s length is not
        equal to zero
            Calculate cruise vector  $C^*$ .
            Calculate step vector  $\Delta x$ .
            Update position.
    
```

2.4 Calculation model and analysis of AFPM

Single-gap axial flux slotted machine is considered for analysis. For clarity, one stator and its rotor with magnets is shown in fig 2 and 3.

The calculation model is by dividing the AFPM into elementary machines linear machines.[8] [9]. The magnets are sinusoidally formed permanent magnets and divided into n sector of rings radially. The overall performance is the sum of individual linear machines. For better accuracy in performance prediction, the number of elementary machines may be increased. In the present analysis, ten number of linear machines are considered. For each computational plane, the diameters, pole pitch, magnet width are computed. Flux density in the air gap for all elementary machine is plotted and analyzed. The performance of all linear machines is computed.

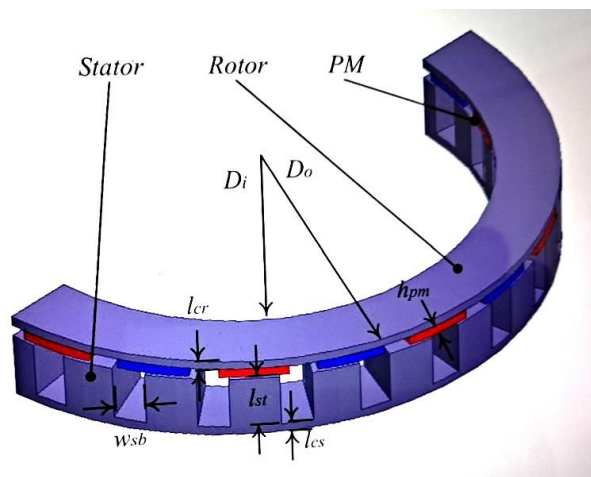


Fig. 6 Machine dimensions

2.5 Airgap

While calculating the flux density in the air gap, it is necessary to consider the effect of stator slot opening and the effect of magnet. [10]

$$g_e = K_c g' \quad (6)$$

$$g' = \left(g + \frac{h_m}{\mu_r} \right) \quad (7)$$

$$K_c = \left[1 - \frac{w_s}{\tau_s} + \frac{4g'}{\pi\tau_s} \ln \left(1 + \frac{\pi w_s}{4g'} \right) \right]^{-1} \quad (8)$$

where

K_c = Carters coefficient.

w_s = slot opening lip width

τ_s = slot pitch

g' = total air gap length

μ_r = relative permeability

h_M = magnet thickness.

2.6 Magnetic field distribution

To make the analysis simple, the axial flux machine is handled as a linear motor. The analytical expression for air gap flux density at the interface of the airgap and armature at $y = g'$ is given by the following expression [8],[9].

$$B_{PM(x)} = \sum_{n=1,3,5}^{\infty} \left(\frac{8B_r}{n\pi} \sin \left(\frac{n\pi\alpha_{PM}m_i}{2} \right) \right) \frac{\left(e^{\frac{-2n\pi\delta}{\tau_{p,ni}}} + 1 \right) + \frac{\mu_m \left(e^{\frac{-2n\pi\delta}{\tau_{p,ni}}} + 1 \right) \cdot \left(e^{\frac{2n\pi h_{PM}}{\tau_{p,ni}}} + 1 \right)}{\mu_0 \left(e^{\frac{2n\pi h_{PM}}{\tau_{p,ni}}} - 1 \right)}}{e^{\frac{-n\pi\delta}{\tau_{p,ni}}} \cos \left(\frac{n\pi x}{\tau_{p,ni}} \right)} \quad (9)$$

Where B_r = remanent magnetic flux density

μ_0 = free space recoil permeability

μ_M = PM recoil permeability

τ = pole pitch

η = magnet width/ pole pitch

h_M = magnet height (thickness)

n = Harmonic order

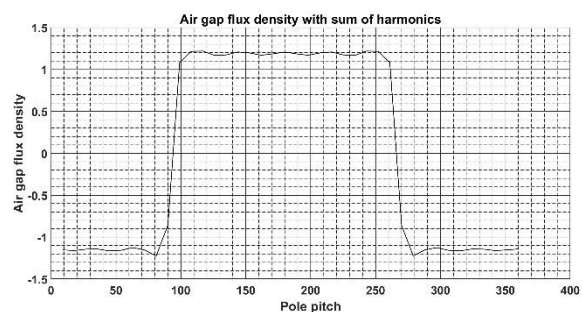


Fig 7. Air gap flux density considering all harmonics.

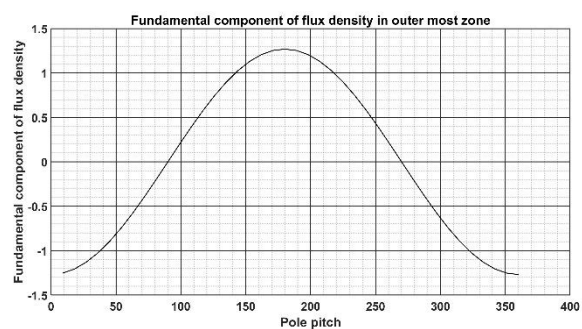


Fig 8. Fundamental component of flux density in outer zone.

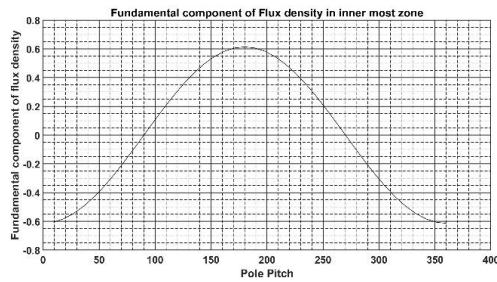


Fig 9. Fundamental component of flux density in Inner most zone.

2.7 Voltage dip due to stator slot opening

The drop in flux density ($B_{max} - B_{min}$) is calculated using the following: [8].

$$B(\alpha) = \left(1 - 2 \cdot \beta \sin^{2n} \frac{\pi}{\alpha_d} \alpha\right) \cdot B_{max} \quad (10)$$

α_d is the angle ($0 \dots \pi$) corresponding to slot pitch τ_s . The depth of the drop in flux density is ($B_{max} - B_{min}$).

$$n = \frac{\tau_s - w_{so}}{w_{so}} \quad (11)$$

$$u = \frac{w_{so}}{2\delta} + \sqrt{1 + \left(\frac{w_{so}}{2\delta}\right)^2} \quad (12)$$

$$\beta = \frac{(B_{max} - B_{min})}{2B_{max}} \quad (13)$$

$$\beta = \frac{1 + u^2 - 2u}{2 \cdot (1 + u^2)}$$

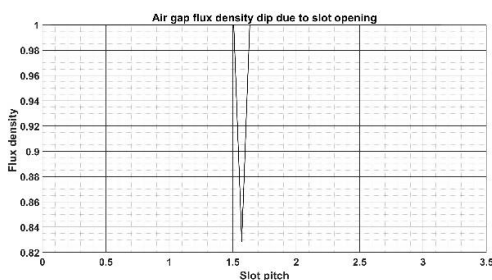


Fig 10. Air gap flux density dip due to stator slot opening.

2.8 Magnetic flux

The average magnetic flux Φ_f inside the gap is given by [5]

$$\Phi_f = \int_{r_{in}}^{r_{out}} \alpha_i B_{mg} \frac{2\pi}{p} r dr \quad (14)$$

$$= \alpha_i B_{mg} \frac{\pi}{2p} (r_{out}^2 - r_{in}^2) \quad (15)$$

Where α_i is pole width to pole pitch ratio, B_{mg} is peak flux density, p is pairs of poles and r_{out} and r_{in} are outer and inner radius of the machine.

2.9 Torque and Torque constant (K_t) [5]

The rms value the torque is given by

$T = K_t I_a$ where K_t is torque constant.

$$K_t = \frac{m}{\sqrt{2}} p N_1 k_{w1} \Phi \quad (16)$$

2.10 EMF constant (K_{emf}) [5]

The rms value E_f induced in one phase is given by

$$E_f = K_{emf} \cdot n_s \quad (17)$$

where K_{emf} is EMF constant and is given by

$$K_{emf} = \pi \sqrt{2} p N_1 K_{w1} \Phi \quad (18)$$

n_s speed in revolutions per second.

2.11 Turns per phase (N_1) [5]

The turns per phase may be given by

$$N_1 = \frac{\pi D_{out} (1 + k_d) A_m}{4m\sqrt{2} I_a} \quad (19)$$

$$k_d = \frac{r_{in}}{r_{out}} \quad (20)$$

Where A_m is electrical loading and k_d is the ratio between the outer radius and inner radius of the machine and D_{out} is the outer diameter of the stator.

2.12 Magnet shape

To minimize the cogging torque and noise, magnets are traditionally skewed. By magnet shaping to sinusoidal wave shape, it is possible to reduce the cogging effect [11]. The outline of the magnet, for fundamental component sinusoidal wave may be given by the following equation.

$$y(x) = h \cdot \sin\left(\frac{\pi x}{w}\right) \quad (21)$$

where h is the height of magnet and w is the length of magnet shape.

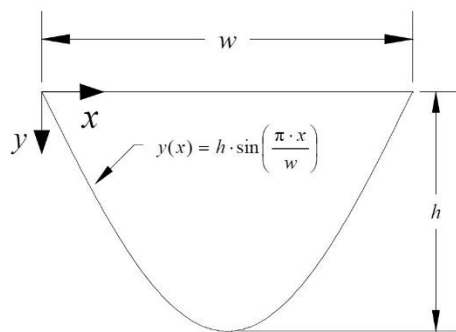


Fig 11. Sinusoidal magnet shape

2.13 Optimized model details

As explained in sec 2.4, machine is divided into ten radial sector of rings of elementary machines. For increasing the computational accuracy, the number of elementary machines may be increased from 10. The permanent magnet profile is shaped sinusoidal. Each elementary machine has individual permanent magnet width with respect to its pole pitch. The pole pitch of elementary machine of P poles equals to

$$\tau_i = \pi * (R_i + R_{i+1}) / P \quad (22)$$

τ_i = pole pitch in i^{th} ring
 R_i = inner radius of i^{th} ring
 R_{i+1} = outer radius of i^{th} ring

The magnet width to pole pitch ratio is decided by optimized variable - magnet width pole pitch ratio.

Variable	Max	Min
Outer diameter (mm)	490	340
Diameter ratio (Inner /outer)	0.7	0.6
Air-gap(mm)	1.5	0.5
Current density (amp/mm ²)	10	6
Magnet width / Pole pitch	0.9	0.6
Magnet thickness/ Pole pitch	0.125	0.042

Table 5
Machine Data

Parameter [unit]	Value
Nominal output (kW)	80
Nominal Torque (Nm)	254
Number of slots	18
Speed (RPM)	3000
Number Poles	16

Remanent Magnetic flux density (Br)	1.2
Number of stators	1
Phase to star point voltage (Volts)	163

2.14 Torque density

The machine torque density is defined as [12]

$$\tau_{den} = \frac{P_{out}}{\omega_m \frac{\pi}{4} D_{tot}^2 L_{tot}} \quad (23)$$

τ_{den} = Torque density [N.m/cm³]

ω_m = angular speed [Rad/s]

D_{tot} = machine outer diameter total [m]

L_{tot} = machine axial length total [m]

P_{out} = rated power [W]

Table VI
Optimized motor diameters
parameters and Peak flux density
(T)

Parameter	OD(m)	Peak Bg T (Sin)
Zone 1	0.338	1.287
Zone 2	0.328	1.330
Zone 3	0.318	1.368
Zone 4	0.308	1.400
Zone 5	0.298	1.423
Zone 6	0.289	1.430
Zone 7	0.277	1.410
Zone 8	0.267	1.343
Zone 9	0.257	1.183
Zone 10	0.247	0.785

3.Optimized results

Table VII	
Optimized machine parameters	
Parameter	Value
Outer diameter (mm)	338.7
Air gap (mm)	1.5
Inner diameter (mm)	237.1
Magnet Thickness (mm)	4.76
Magnet width/ Pole pitch	0.6
Number of stators	1
Number of turns per phase	12
Torque constant	0.6277
Conductor area (mm ²)	57.95
Slot width at bottom (mm)	38.38
Slot height (winding portion)	49.8
Slot lip opening width	3
Slot lip opening height	1
Number of slots	18
Winding DC resistance/phase (ohms)	0.00217
Machine axial length (mm)	102.8
(Output/Weight) ratio (kW/kg)	2.24
Efficiency %	98%

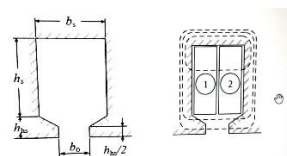


Fig 12. Winding slot details

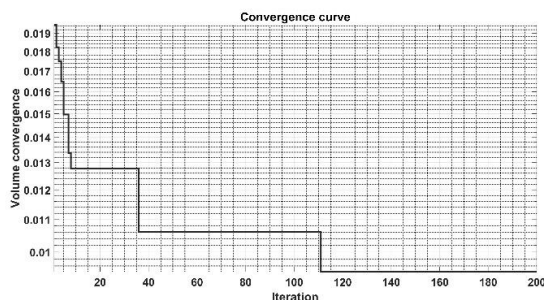


Fig 13. Convergence curve of GEO optimization

III. Conclusions

Golden Eagle Optimizer is a useful optimization tool. This program is relatively easy to use with MATLAB. There are many configurations available in AFPM motors. In this paper a simple configuration ie single stator model is used. GEO can be extended to optimize parameters in other

configurations. Further, in this paper an optimization is done for a single objective. But in practice, multi objective optimization are to be done. GEO can be extended to other configurations and multi objectives.

Acknowledgements

The author wishes to thank Ms. Sri Rekha Mamidi for her sincere help in preparing the paper and presentation to confirm requirements.

BIOGRAPHIES

Author has done his Masters Degree in Electrical Engineering with specialization in Rotating Electrical Machines from Indian Institute of Technology , IIT (Mumbai) in 1970. His interests are in the field of 'design of large electrical machines, Optimization and Machine learning. He has presented technical papers in national and international conference and published in journals.

References

- [1] Massimiliano Gobbi *, Aqeab Sattar , Roberto Palazzetti , Gianpiero Mastinu: "Traction motors for electric vehicles: Maximization of mechanical efficiency – A review". <https://www.sciencedirect.com/science/article/pii/S0306261923018603> 27 pages, ELSEVIER
- [2] Electric Vehicle Database. <https://ev-database.org/car/1019/Nissan-Leaf-24-kWh>
- [3] Mahmoud M Akl, Abdelsalam A Ahmed, Essam Eddin M Rashad : "A Wide Component Sizing and Performance Assessment of Electric Drivetrains for Electric Vehicle" https://www.researchgate.net/publication/338543178_A_Wide_Component_Sizing_and_Performance_Assessment_of_Electric_Drivetrains_for_Electric_Vehicles#fullTextFileContent, 2019 21st International Middle East Power systems Conference, Tanta University, Egypt , IEEE
- [4] A. Mahmoudi, N A Rahim and WP Hew : "Axial-flux permanent magnet machine modeling design, simulation and analysis". University of Malaya, Malaysia. <http://www.academicjournals.org/SRE>, ISSN 1992-2248 Academic journals pages26
- [5] Francesco La Greca : " Master Degree in Electrical Engineering Design of axial flux motors for automotive purpose" .

<https://webthesis.biblio.polito.it/18952/1/tesi.pdf> AY 2021/2022 Politecnico Di Torino, pages 115

[6] Abdolkarim Mohammadi-Balani : “Golden Eagle

Optimizer A Nature-Inspired Metaheuristic Algorithm.” *Computers & Industrial Engineering*, vol.152, Elsevier BV, Feb. 2021, p. 107050,doi:10.1016/j.cie.2020.107050.

<https://www.mathworks.com/matlabcentral/fileexchange/84430-golden-eagle-optimizer-toolbox>.

[7] Abdolkarim Mohammadi-Balani , Mahmoud

Dehghan Nayeri, Adel Azar, Mohammadreza Taghizadeh – Yazdi: “Golden Eagle Optimizer: A nature inspired metaheuristic algorithm”.

<https://doi.org/10.1016/j.cie.2020.107050>, Tarbiat, Modares University, Tehran, Iran , 45 page

[8] Panu Kurronen, Juha Pyrhonen: “Analytic

Calculation of an Axial-Flux Permanent Magnet Motor Torque”

https://www.academia.edu/16251290/Analytic_calculation_of_axial_flux_permanent_magnet_motor_torque Lappeenranta University of Technology, Department of Electrical Engineering, P.O.Box 20, 53850 Lappeenranta, Finland, 12 pages. Source IEEE Xplore .

[9] Asko Parvianen, Markku Niemela and Juha Pyrhonen: “ Modeling of Axial flux permanent

Magnet Machines”. *IEEE transactions on Industry applications*, Lappeenranta – Lathi University of Technology, LUT October 2004, publication at: <https://www.researchgate.net/publication/3171832>

[10] Myung-Jin, Dae-Gab Gweon: “Modeling of the

armature slotting effect in the field distribution of a linear permanent magnet motor”.

<https://www.scribd.com/document/665839777/Archiv-fur-Elektrotechnik-2002-may-01-vol-84-iss-2-Myung-Jin-Chung-Dae-Gab-Gweon-Modeling-of-the-armature-slotting-effect-in-the-magnetic-field> , *Electrical Engineering* 84 (2002) 101-108, Springer Verlag 2002, 8 pages.

[11] A. Paviainen, J. Pyrhonen, M. Niemela: “ Axial

flux interior permanent magnet Synchronous motor with sinusoidally shaped magnets;

<https://www.researchgate.net/publication/239831528> 10th International Symposium on Electromagnetic Fields in Electrical Engineering Cracow, Poland, September 20-22, 2001. Lappeenranta University of Technology, Department of Electrical Engineering, Finland, 6 Pages

[12] A. Mahmoudi, N A Rahim and H W Ping : “ Axial

Flux Permanent Magnet Motor Design for Electric

Vehicle Direct Drive using sizing equation and Finite element analysis.” *University of Malays, Kuala Lumpur. Progress in Electromagnetic Research*, Vol 122, 467-496, 2012